

The gravitational wave and short gamma-ray burst GW170817/SHB170817A, not your everyday binary neutron star merger

A. De Rújula

Instituto de Física Teórica (UAM/CSIC), Univ. Autónoma de Madrid, Spain;
Theory Division, CERN, CH 1211 Geneva 23, Switzerland¹

Abstract

This event, so far unique, beautifully confirmed the standard views on the gravitational waves produced by a merger of two neutron stars, but its electromagnetic multi-wavelength observations disagreed with the numerous initial versions of the “standard fireball model(s)” of gamma ray bursts. Contrariwise, they provided strong evidence in favour of the “cannonball” model. Most uncontroversially, a cannonball was observed at radio wavelengths, with an overwhelming statistical significance ($> 17\sigma$), and travelling in the plane of the sky, as expected, at an apparent superluminal velocity $V_{app} \sim 4c$.

Keywords: Gravitational waves; Gamma ray bursts; Neutron star mergers; Afterglows; Supernovae; Cannonballs; Fireballs.

1. Introduction

The GW170817 event was the first binary neutron-star merger detected with Ligo-Virgo [1] in gravitational waves (GWs). It was followed by SHB170817A¹, 1.74 ± 0.05 s after the end of the GW’s detection. The SHB’s afterglow across the electromagnetic spectrum was used to localize its source [2] to the galaxy NGC 4993, at a cosmologically very modest redshift, $z = 0.009783$. The GW170817/SHB170817A association was the first indisputable confirmation that pairs of neutron stars merging due to GW emission produce GRBs, thereafter converting this suggestion [3] [4] into a general consensus.

Less generally well known is the fact that two days before the discovery date, a paper appeared on arXiv [5], not only reiterating the neutron star merger hypothesis, but predicting that a SHB found in combination with a GW would be seen far off axis. The prediction was based on the much greater red-shift reach of GRB or SHB observations relative to the GW ones and the fact that the γ rays are extremely collimated. Thus, within the volume reach of GW observations, it would be most unlikely for a SHB to point close to the observer.

Since 1997 only two theoretical models of GRBs and their afterglows (AGs) –the standard fireball (FB) model [6] and the cannonball (CB) model [7]– have been extensively used to interpret the innumerable observations. Advocates of both models have claimed to fit the data very well. But the two models

were originally and still are quite different in their basic assumptions, despite the repeated replacements of key assumptions of the “standard” FB model (but not its name) with assumptions underlying the CB model (e.g. supernovae of Type Ia as progenitors of most GRBs, highly collimated ejecta made of ordinary matter, as opposed to spherical or conical shells of an $e^+e^- \gamma$ plasma, “jets” not necessarily seen almost on axis). For a recent extensive discussion of the observational tests of FB and CB models, see [8].

Significantly, and in contrast to the FB model(s), the CB model has made many successful *predictions*. Among them, the large polarization of the GRB’s γ rays [9], the precise date at which the supernova associated with GRB030329 would be discovered [10], the complex “canonical” shape [11] of many GRB afterglows [12, 13], the correlations between various prompt² observables amongst them [14, 15] or with AG observables [16].

The SHB170817A event is an optimal case to tighten the discussion of the comparisons between different models of GRBs. The question of the apparently superluminal motion of the source of its afterglow, discussed in chapter 7, is particularly relevant.

2. The cannonball model

The CB model is based on a straightforward analogy of a phenomenon that is abundantly observed but poorly understood: the relativistic ejecta emitted by quasars and micro-quasars. The model [9] is illustrated in Figure 1. In it, bipolar jets of highly relativistic ordinary-matter plasmoids (a.k.a. CBs)

Email address: alvaro.derujula@cern.ch (A. De Rújula)

Instituto de Física Teórica (UAM/CSIC), Univ. Autónoma de Madrid, Spain;
Theory Division, CERN, CH 1211 Geneva 23, Switzerland)

¹SHB stands for “Short Hard Burst”, a sub-class of gamma-ray bursts (GRBs) lasting less than ~ 2 s and whose photons generally have comparatively large energies.

²Prompt customarily refers to quantities measured prior to the afterglow phase. Naturally, the distinction is not always sharp.

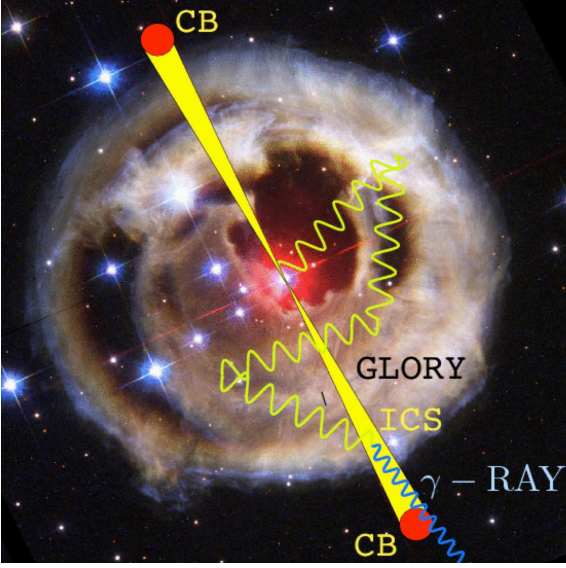


Figure 1: Electrons in a cannonball inverse Compton scatter photons in the glory of light surrounding a newly-born compact object, launching them forward as a narrow beam of γ rays.

are assumed to be launched as a compact stellar object is being born. SNe of Type Ic (the broad-line stripped-envelope ones) thus generate long-duration GRBs by the electrons in a CB raising the photons in the SN's "glory" by Inverse Compton Scattering (ICS) into a forward-collimated narrow beam of γ -rays [9].

Similarly, in the CB model, mergers of two neutron stars (NSs) or a NS and a black hole (BH) give rise to SHBs. In this case, the role of the glory of light is played by a Pulsar Wind Nebula (PWN) powered by the spin-down of a newly born rapidly-rotating pulsar— suggesting that most SHBs are produced by NS mergers yielding a NS remnant rather than a black hole [17, 18]. SN-less GRBs are produced in high-mass X-ray binaries, as a NS accreting mass from a companion suffers a phase transition to a denser object. Finally X-ray flashes (XRFs) and some X-ray transients are simply GRBs observed from a relatively large angle relative to the CBs' emission axis.

3. Is SHB170817A noteworthy all by itself?

A first question regarding SHB170817A is whether or not it is a typical SHB. The CB model provides a strongly affirmative answer, in all respects. A first test employs the correlations between observables predicted by this model.

Let γ_0 be the initial Lorentz factor with which a CB is launched. Its electrons inverse-Compton-scatter the ambient photons they encounter. This results in a γ -ray pulse of aperture $\simeq 1/\gamma_0 \ll 1$ around the CB's direction. Viewed by an observer at an angle θ relative to the CB's direction, the individual photons are boosted in energy by a Doppler factor $\delta_0 \equiv \delta(t=0) = 1/[\gamma_0(1-\beta_0 \cos \theta)]$ or, to a good approximation for $\gamma_0^2 \gg 1$ and $\theta^2 \ll 1$, $\delta_0 \simeq 2\gamma_0/(1+\gamma_0^2\theta^2)$.

The ICS of photons of energy ϵ by a CB boosts their energy, as seen by an observer at redshift z , to $E_\gamma = \gamma_0 \delta_0 \epsilon / (1+z)$. Con-

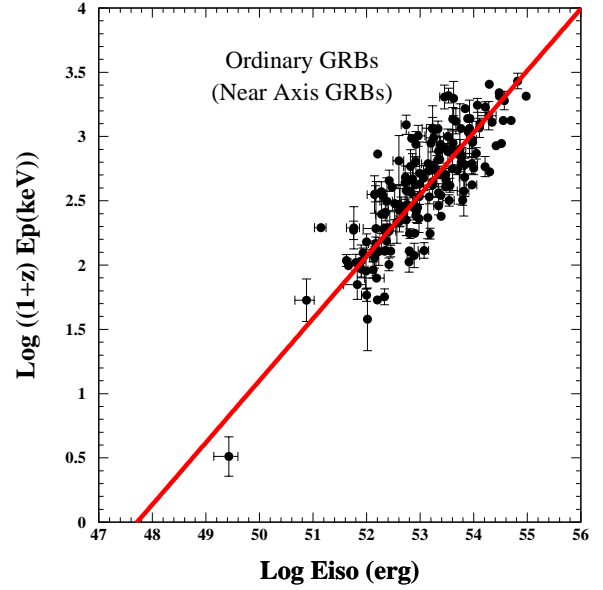


Figure 2: The $[E_p, E_{iso}]$ correlation in ordinary LGRBs viewed near axis. The line is the best fit, whose slope, 0.48 ± 0.02 , agrees with the CB model prediction of Equation 3. The lowest E_{iso} GRB is 020903 at $z=0.25$ (HETE).

sequently, the peak energy, E_p , of their time-integrated energy distribution satisfies

$$(1+z) E_p \approx \gamma_0 \delta_0 \epsilon_p, \quad (1)$$

with ϵ_p the characteristic or peak energy of the initial photons (for the glory of a SN $\epsilon_p \sim O(1)$ eV, for a PWN $\epsilon_p \sim O(1)$ keV).

In the Thomson regime the nearly isotropic distribution (in the CB's rest frame) of a total number n_γ of IC-scattered photons is beamed into an angular distribution $dn_\gamma/d\Omega \approx (n_\gamma/4\pi)\delta^2$ in the observer's frame. Consequently, the isotropic-equivalent total energy of the photons satisfies

$$E_{iso} \propto \gamma_0 \delta_0^3 \epsilon_p. \quad (2)$$

Hence, both ordinary long- and short-duration GRBs, viewed most probably from an angle $\theta \approx 1/\gamma$ (for which $\delta_0 \approx \gamma_0$), are predicted [14] to satisfy the "Amati" correlation [19],

$$(1+z) E_p \propto [E_{iso}]^{1/2}, \quad (3)$$

shown in Figure 2.

Far off-axis GRBs [$\theta^2 \gg 1/\gamma^2$, so that $\delta_0 \approx 2/(\gamma_0 \theta^2)$], have a much lower E_{iso} , and satisfy

$$(1+z) E_p \propto [E_{iso}]^{1/3}. \quad (4)$$

As one can see in Figure 3, SHB170817A "is right where it should be". As we shall discuss anon, it was indeed seen far off-axis.

In the CB model the peak-time of a single γ -ray pulse obeys $T_p \propto (1+z)/\gamma_0 \delta_0$, and its peak energy, E_p , is that of Equation 1. SHB170817A, being a one-peak event, is a good case to

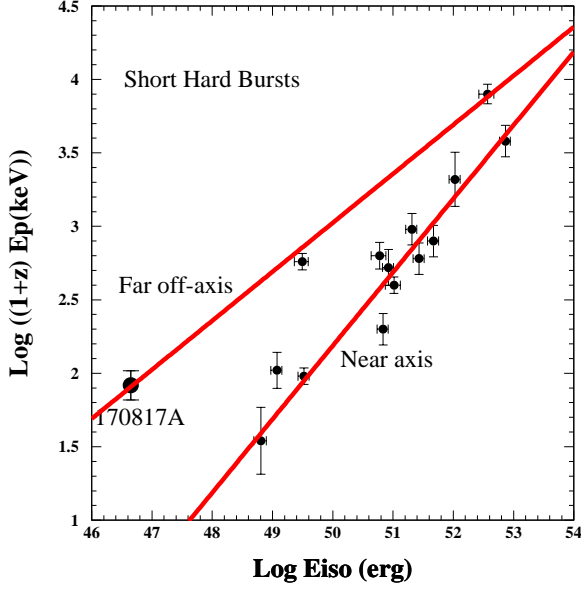


Figure 3: The $[E_p, E_{iso}]$ correlations in SHBs. The lines are the CB model predicted correlations as given by Equations 3 and 4.

study these observables. Indeed, one of the simplest CB-model predictions is the $[E_p, T_p]$ correlation $E_p \propto 1/T_p$. In Figure 4 this correlation is compared with the values of E_p and T_p in the GCN circulars [20] for resolved SGRB pulses. Again, SHB170817A is where it should be.

A more detailed test concerning the run-of-the-mill nature of SHB170817A is the shape of its single pulse of γ 's. The light “reservoir” that a CB will Compton up-scatter (a SN glory or a PWN) has a thin thermal bremsstrahlung spectrum and a number density distribution decreasing with distance to the CB source as $1/r^2$ [21]. With these inputs it is straightforward to derive a two-parameter simple expression that provides excellent descriptions of pulse shapes [22]. A particularly well measured GRB pulse is shown in Figure 5.

The pulse of SHB170817A is shown in Figure 6. Once more, there is nothing atypical about it.

3.1. Prompt observables of SHB170817A. Further checks

Initial Lorentz factor. In the CB model GRBs and SHBs can be understood as approximately standard candles viewed from different angles. As illustrated in Figure 3, low luminosity (LL) SHBs such as SHB170817A are ordinary (O) SHBs, but viewed far off-axis. Consequently, their E_{iso} and E_p are expected to obey the relations

$$E_{iso}(\text{LL SHB}) \approx \langle E_{iso}(\text{O SHB}) \rangle / [\gamma^2 (1 - \cos \theta)]^3, \quad (5)$$

$$(1 + z) E_p(\text{LL SHB}) \approx \langle (1 + z) E_p(\text{O SHB}) \rangle / [\gamma^2 (1 - \cos \theta)]. \quad (6)$$

Given the measured value $E_{iso} \approx 5.4 \times 10^{46}$ erg of SHB170817A [23], the mean value $\langle E_{iso} \rangle \approx 1 \times 10^{51}$ erg of ordinary SGRBs, and the viewing angle $\theta \approx 28$ deg obtained—as

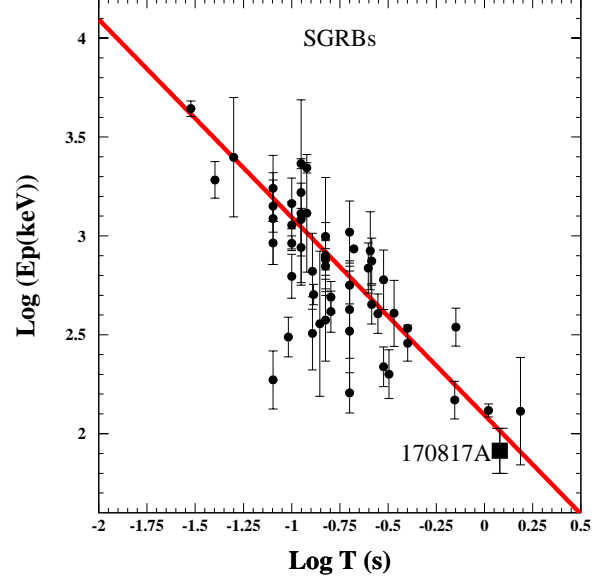


Figure 4: Comparison between the predicted correlation ($E_p \propto 1/T_p$) and the corresponding data in GCN circulars for 54 resolved pulses of SGRBs, obtained by the Konus-Wind and Fermi-GBM collaborations.

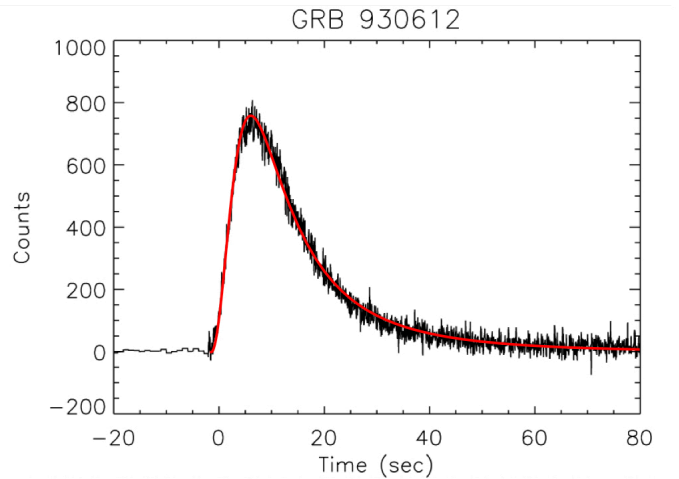


Figure 5: The pulse shape of GRB930612 measured with BATSE aboard CGRO and the best CB-model fit to re-binned data [24]

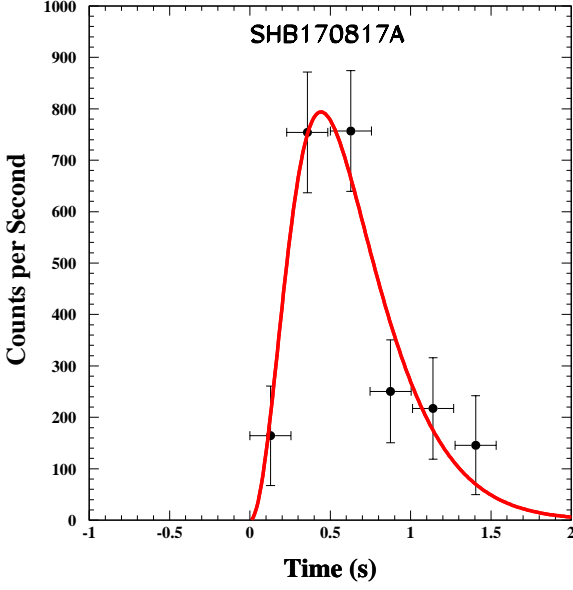


Figure 6: The pulse shape of SHB170817A measured with the Fermi-GBM [26, 27, 28, 29, 30] and its CB-model best fit, with $\chi^2/\text{dof} = 0.95$ [24].

we shall discuss in detail in section 7.1– from the superluminal motion of the source of the radio AG of SHB170817A [25], Equation 6 yields $\gamma_0 \approx 14.7$ and $\gamma_0 \theta \approx 7.2$.

With γ_0 and θ specified, Equations 5 and 6, result in the following additional tests of CB model predictions:

Peak energy. Assuming that SHBs have the same redshift distribution as GRBs (with a mean value $\langle z \rangle \approx 2$), and given the observed $\langle E_p \rangle = 650$ keV of SHBs [23], one obtains $\langle (1+z) E_p \rangle \approx 1950$ keV. Consequently, Equation 6 with $\gamma_0 \theta \approx 7.2$ and $z \approx 1$ yields $E_p \approx 75$ keV for SHB170817A. This is to be compared with $E_p = 82 \pm 23$ keV (T_{90}) reported in [26], $E_p = 185 \pm 65$ keV estimated in [27], and $E_p \approx 65 + 35(-14)$ keV estimated in [28], from the same data, with a mean value $E_p = 86 \pm 19$ keV, agreeing with the expectation.

Peak time. In the CB model the peak time Δt after the beginning of a GRB or SHB pulse is roughly equal to half of its full width at half maximum (FWHM) [22]. Assuming again that SHBs are roughly standard candles, the dependence of their Δt values on θ is

$$\Delta t(\text{LL SHB}) \approx \gamma_0^2 (1 - \cos \theta) \langle \Delta t(\text{O SHB}) \rangle, \quad (7)$$

For $\theta \approx 28$ deg, $\Delta t \approx 0.58$ s obtained from the prompt emission pulse of SHB170817A (see Figure 6), and $\langle \text{FWHM}(\text{SHB}) \rangle = 55$ ms, Equation 16 results in $\gamma_0 \approx 14.7$. Using Equations 5 and 6, and $\gamma_0 \theta \approx 7.2$ one checks that this value of γ_0 is consistent with $E_{\text{iso}} = 5.4 \times 10^{46}$ estimated in [31], and $\langle E_p \rangle = 86 \pm 19$ keV the mean of the estimates in [17].

In the CB model the shape of resolved SHB and GRB pulses satisfies $2 \Delta t \approx \text{FWHM} \propto 1/E_p$, as illustrated in Figure 4. Using the observed $\langle \text{FWHM}(\text{SHB}) \rangle \approx 55$ ms, $\gamma_0 \approx 14.7$, and $\theta \approx 28$ deg, Equation 7 for SHB170817A results in $\Delta t \approx 0.63$ s, in good agreement with its observed value, 0.58 ± 0.06 s.

Quite obviously, the replacements we have been making of physical parameters by their means may not be completely reliable, not only because of the spread in their values, but also because of detection thresholds and selection effects. Yet, in checking the unexceptional nature of SHB170817A, they work better than one could expect.

4. SHB170817A in FB models, prompt observables

The correlations in Figures 3,4 are trivial consequences of GRBs being narrow beams of γ rays seen somewhat off-axis. They are not predictions of FB models. In them, the jetted beams were generally assumed to be seen on-axis, at least up to the observation of SHB170817A.

In FB models [6] the GRB prompt pulses are produced by synchrotron radiation from shock-accelerated electrons in collisions between overtaking thin shells ejected by the central engine, or by internal shocks in the ejected conical jet. Only for the fast decline phase of the prompt emission, and only in the limits of very thin shells and fast cooling, falsifiable predictions have been derived [32, 33, 34]. They result in a power law decay $F_\nu(t) \propto (t - t_i)^{-(\beta+2)} \nu^{-\beta}$, where t_i is the beginning time of the decay phase, and β is the spectral index of prompt emission. The observed decay of the SHB170817A pulse could only be reproduced by adjusting a beginning time of the decay and replacing the constant spectral index of the FB model by the observed time-dependent one [32].

The multitude of tests discussed in section 3.1 are only based on Compton scattering and relativistic kinematics for approaching objects seen significantly off-axis, like the prompt-observable correlations we discussed. They do not belong to FB models.

5. The afterglow of GRBs and SHBs

In the CB model the afterglow of GRBs is due to synchrotron radiation (SR) from the electrons in a CB that is traveling and decelerating as it interacts with the interstellar medium (ISM), previously fully ionized by the GRB's γ rays. The electrons radiate in the turbulent magnetic field generated by the merging plasmas, whose energy density is assumed to be in equilibrium with the kinetic energy brought (in the CB's rest system) by the ISM constituents. With these inputs, the model provides an excellent and predictive description of the temporal and spectral dependence of GRB afterglows.

The CB-model's description of the early AGs of “Supernova-less” GRBs and SHBs differs from the one of ordinary (SN-generated) GRBs. It is simply the isotropic radiation from a pulsar wind nebula (PWN), powered by a newly born rapidly-rotating pulsar, and has an expected luminosity [35] satisfying

$$L(t, t_b)/L(t=0) = (1 + t/t_b)^{-2}, \quad (8)$$

with $t_b = P(0)/2 \dot{P}(0)$, where $P(0)$ and $\dot{P}(0)$ are the pulsar's initial period and its time derivative.

The *universal behaviour* [36] of Equation 8 describes well the AG of all the SN-less GRBs and SHBs with a well sampled

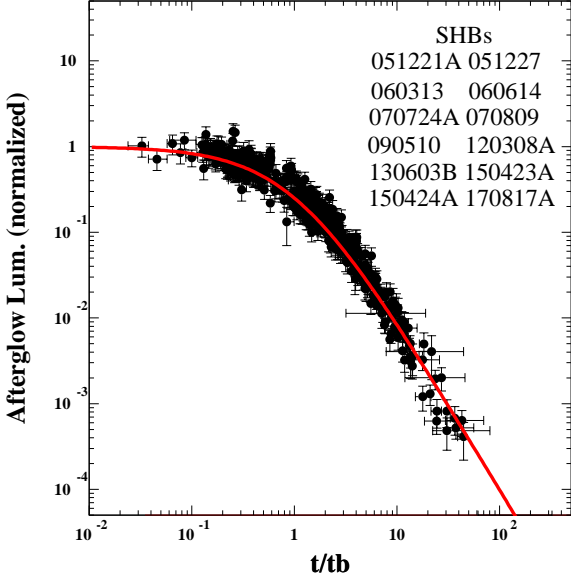


Figure 7: Comparison between the normalized light curve of the X-ray AG of 11 SHBs with a well sampled AG measured with Swift’s XRT [37] during the first couple of days after burst and the predicted universal behavior of Equation 8. The bolometric light curve of SHB170817A [38] is included, and shown separately in Figure 8.

AG during the first few days after burst. This is demonstrated in Figure 7 for the twelve SHBs [17] from the Swift XRT light curve repository [37] that were well sampled in the mentioned period.

The bolometric light curve of SHB170817A [38] is shown in Figure 8. The two-parameter [$L(0)$ and t_b] CB-model fit is excellent. SHB170817A, once more time, is not deviant.

5.1. The late-time afterglow of SHB170817A

The PWN-powered early AG decreases with time extremely fast, as in Figure 8. It is eventually overtaken, in the CB model, by the synchrotron radiation from CBs. In the case of SHB170817A, the AG was particularly well observed up to extremely late times: almost three years [39]. To discuss this subject we need to recall some details.

The observed spectral energy density (SED) flux of the *unabsorbed* SR, $F_\nu(t) = \nu dN_\nu/d\nu$, has the form (see, e.g. Eqs. (28)–(30) in [11]),

$$F_\nu \propto n(t)^{(\beta_x+1)/2} [\gamma(t)]^{3\beta_x-1} [\delta(t)]^{\beta_x+3} \nu^{-\beta_x}, \quad (9)$$

where n is the baryon density of the external medium encountered by the CB at a time t and β_x is the spectral index of the emitted X-rays, $E dn_x/dE \propto E^{-\beta_x}$.

The CBs are decelerated by the swept-in ionized material. Energy-momentum conservation for such a plastic collision³ – between a CB of baryon number N_B , approximately constant

³The original assumption in the CB model was that the interactions between a CB and the ISM were elastic. It was later realized, in view of the shape of AGs at late times, that a plastic collision was a better approximation in the AG phase.

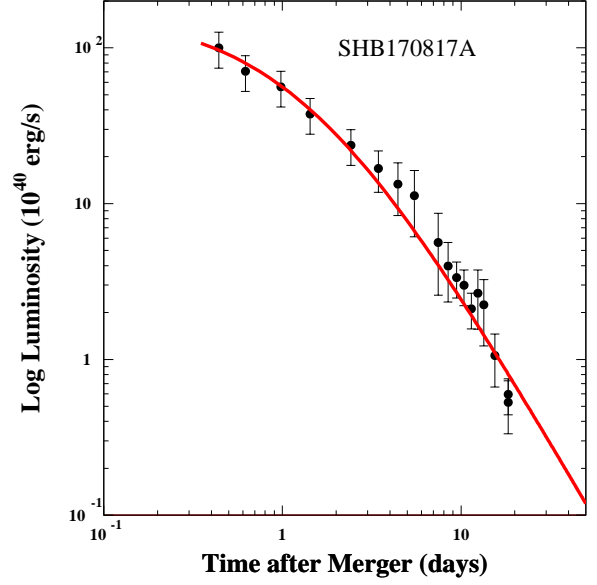


Figure 8: Comparison between the observed [38] bolometric light curve of SHB170817A and the universal light curve of Equation 8, assuming the presence of a milli-second pulsar with $L(0) = 2.27 \times 10^{42}$ erg/s and $t_b = 1.15$ d. The fit has $\chi^2/\text{dof} = 1.04$.

radius R [40], and initial Lorentz factor $\gamma_0 \gg 1$, propagating in an approximately constant-density ISM – implies that the CB decelerates according to [22]:

$$\gamma(t) \simeq \frac{\gamma_0}{\left[\sqrt{(1 + \theta^2 \gamma_0^2)^2 + t/t_d - \theta^2 \gamma_0^2} \right]^{1/2}}, \quad (10)$$

where t is the time in the observer frame since the beginning of the AG emission by a CB, and t_d is its deceleration time-scale:

$$t_d \simeq (1+z) N_B / 8 c n \pi R^2 \gamma_0^3. \quad (11)$$

As long as the Lorentz factor of a decelerating CB is such that $\gamma^2 \gg 1$, $\gamma \delta \approx 1/(1 - \cos \theta)$ and the spectral energy density of its synchrotron AG –Equation 9– can be rewritten as

$$F_\nu(t, \nu) \propto n(t)^{\beta_\nu+1/2} [\gamma(t)]^{2\beta_\nu-4} \nu^{-\beta_\nu}. \quad (12)$$

For a constant density, the deceleration of the CB results in a late-time behavior $\gamma(t) \propto t^{-1/4}$ [16], and as long as $\gamma^2 \gg 1$,

$$F_\nu(t, \nu) \propto t^{0.72 \pm 0.03} \nu^{-0.56 \pm 0.06}, \quad (13)$$

where we used the observed [41] $\beta_\nu = 0.56 \pm 0.06$, which extends from the radio (R) band, through the optical (O) band, to the X-ray band.

If the CB moved out from within a domain of constant internal density into a wind-like density distribution (proportional to r^{-2}) its deceleration rate diminished and $\gamma(t)$ became practically constant. Consequently, the time dependence of F_ν in Equation 12 becomes a fast decline described by

$$F_\nu(t, \nu) \propto t^{-2.12 \pm 0.06} \nu^{-0.56 \pm 0.06}. \quad (14)$$

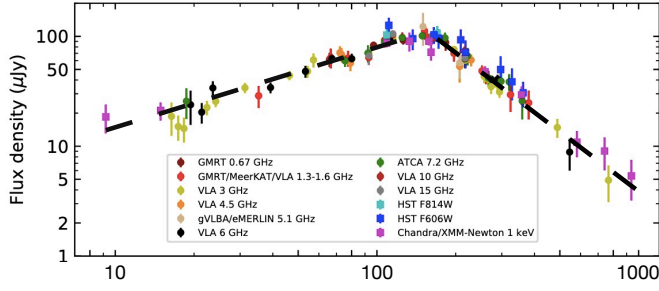


Figure 9: Radio, optical and X-ray observations of the AG of SHB170817A, adapted from Figure 2 of [39]. The horizontal axis is the time after merger, in days. The radio light curve, measured until 940 days post-merger, spans multiple frequencies, and is scaled to 3 GHz using the spectral index -0.584 . The early-time trend expected in the CB model is the rising black-dashed line. The late-time trend, also black-dashed, is for an assumed $1/r^2$ ISM density decline encountered by the CB after day ~ 150 .

These CB-model approximate rise and fall power-law time dependences of the light curves of the ROX afterglow of SHB170817, with temporal indices 0.72 ± 0.03 and -2.12 ± 0.06 , respectively, are in good agreement with the power-law indices extracted in [42], 0.78 ± 0.05 and $-2.41 \pm 0.26 / -0.42$, respectively, in [42]. They also agree with the indices subsequently extracted in [39], 0.86 ± 0.04 and -1.92 ± 0.12 , as shown in Figure 9.

Summarizing: The data in Figure 9 extend from radio to X-ray frequencies and, when corrected with the observed spectral index, satisfactorily lie close to a single curve (the time and frequency dependences of Equations 13 and 14 factorize). The dashed rising trend is the CB-model's prediction for an assumed constant density of the ISM encountered by the CB, which is generally an excellent approximation. The subsequent decline follows from the assumption that, at an observer's time ~ 150 days, the ISM density began to decrease as $1/r^2$. SHB170817A was only exceptional in that the observations lasted long enough for this ISM-density transition to be very clearly observable.

6. FB-model interpretations of SHB170817A

Soon after the discovery of the late-time radio, optical and X-ray afterglows of SHB170817A, many FB model best fits to the initially rising light curves were published. They involved many different models and multiple best-fit parameters (e.g. [43] and references therein). As new observations were made, the proponents of FB model(s) put to use their large flexibility:

In November 2017 the authors of [43] concluded that *The off axis jet scenario as a viable explanation of the radio afterglow of SHB170817A is ruled out* and that a *choked jet cocoon* is most likely the origin of the gamma rays and rising AG of SHB170817A. In October 2018 the authors of [42] reached conclusions opposite to their earlier ones [43, 44] and to their previous arXiv versions. To wit, in [42] they reported a *strong jet signature in the late-time light-curve of GW170817*, and concluded that *while the early-time radio emission was*

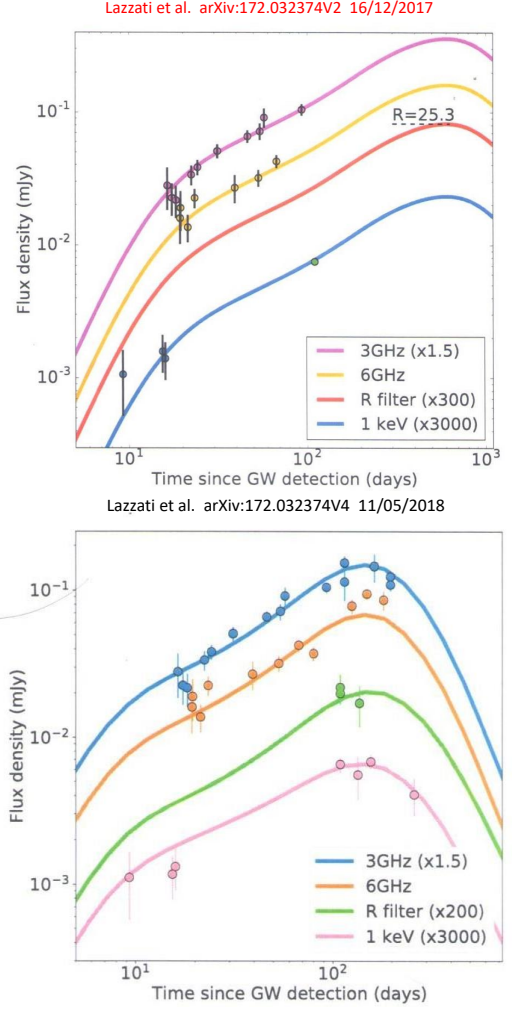


Figure 10: **Above:** Best fit light curves of an off-axis structured jet model [45] to the ROX AGs of SHB170817A measured before December 2017 (Figure from the first version of [45] posted in the arXiv on December 8th, 2017). **Below:** Best fit light curves to the ROX AG of SHB170817A up to April 2018, obtained from a structured jet model [46]. Reported in version 4 of [45] posted in the arXiv on May 11th 2018.

powered by a wider-angle outflow (cocoon), the late-time emission was most likely dominated by an energetic and narrowly-collimated jet, with an opening angle of < 5 degrees, and observed from a viewing angle of about 20 degrees.

All types of FB models –with conical or structured jets– used to fit the multi-band afterglow of SHB170817A failed to correctly predict the subsequent data. This is demonstrated, for example, by the arXiv versions 1-4 of [45] where the evolution of the AG was first incorrectly predicted by a structured jet with a relativistic, energetic core surrounded by slower and less energetic wings, propagating in a low density ISM, as shown in the upper part of Figure 10. When the AG break around day 150 and its subsequent fast decline were observed, the structured jet model with its dozen or so adjustable parameters had no problem to accommodate this behavior, see the lower part of Figure 10.

In the CB model the change of slope in Figures 9 and 10 could not be foretold, but its a-posteriori explanation is simple.

It required changing the ISM density from a constant to a $1/r^2$ behavior, a one-parameter change.

7. The CB's superluminal velocity in GRBs and SHBs

The first observation of an apparent superluminal velocity of a source in the plane of the sky was reported [47] in 1902, and since 1977 in many high-resolution observations of highly relativistic jets launched by quasars, blazars, and micro-quasars. The interpretation of this kind of observation within the framework of special relativity was provided by Paul Courderc in his beautiful article *Les Auréoles Lumineuses des Novae* [48].

A source with a velocity βc at redshift z , viewed from an angle θ relative to its direction of motion and timed by the local arrival times of its emitted photons has an apparent velocity in the plane of the sky:

$$V_{app} = \frac{\beta c \sin \theta}{(1+z)(1-\beta \cos \theta)} \approx \frac{\beta c \gamma \delta \sin \theta}{(1+z)}. \quad (15)$$

For $\gamma \gg 1$, V_{app} has a maximum value $2\gamma c/(1+z)$ at $\sin \theta = 1/\gamma$.

The predicted superluminal velocity of the jetted CBs cannot be verified during the prompt emission phase, because of its short duration and the large cosmological distances of GRBs. But the superluminal velocity of the jet in far off-axis, i.e. nearby low-luminosity SHBs and GRBs, can be obtained from high resolution follow-up measurements of their AGs [49]. Below, two cases are treated in detail: SHB170817A and GRB030329.

7.1. The superluminally moving source of SHB170817A

The VLBI/VLBA observations of the radio AG [25] of SHB170817A provided images of an AG source escaping from the GRB location with superluminal celerity. Such a behavior in GRBs was predicted within the CB model [7] two decades ago [25].

Figure 11, borrowed from [25], shows the displacement with time of a compact radio source. The figure displays the angular locations of the radio source of the AG of SHB170817A moving away in the plane of the sky from the SHB location by 2.68 ± 0.3 mas between day 75 and day 230. In [25] this image is called “a jet”. It is in fact a time-lapse capture of the moving CB emitted (approximately) towards us by the fusion of the neutron stars.

We have estimated that, for the CB responsible for SHB170817A, $\gamma \sim 14.7$, that is $\beta \sim 0.998$. In the excellent $\beta = 1$ approximation one may rewrite Equation 15, and express in terms of observables as:

$$V_{app} \approx \frac{c \sin \theta}{(1+z)(1-\cos \theta)} \approx \frac{D_A \Delta \theta_s}{(1+z)\Delta t}, \quad (16)$$

where $\Delta \theta_s$ is the angle by which the source is seen to have moved in a time Δt . The angular distance to SHB170817A to its host galaxy NGC 4993, at $z = 0.009783$ [2], is $D_A = 39.6$ Mpc, for the local value $H_0 = 73.4 \pm 1.62$ km/s Mpc obtained from Type Ia SNe [50]. The location of the VLBI-observed source – which moved $\Delta \theta_s = 2.70 \pm 0.03$ mas in a time $\Delta t = 155$ d (between

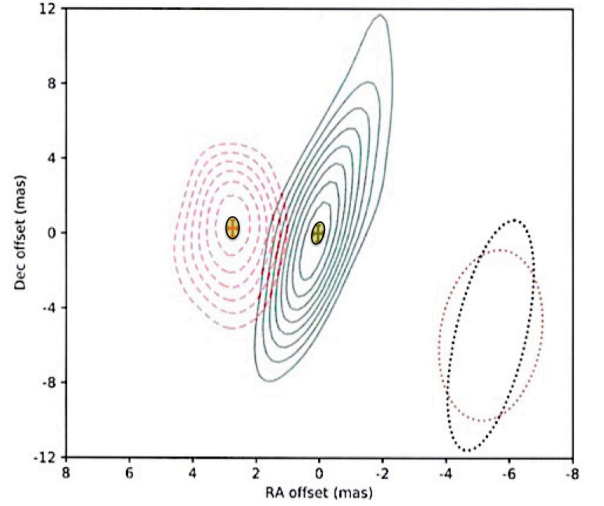


Figure 11: Proper motion of the radio counterpart of GW170817. Its authors [25] explain: *The centroid offset positions (shown by 1σ error bars) and 3σ – 12σ contours of the radio source detected 75 d (black) and 230 d (red) post-merger with VLBI at 4.5 GHz. The radio source is consistent with being unresolved at both epochs. The shapes of the synthesized beam for the images from both epochs are shown as dotted ellipses in the lower right corner. The proper motion vector of the radio source has a magnitude of 2.7 ± 0.3 mas. The 1σ domains have been colored not to deemphasize the effectively point-like (unresolved) nature of the source (a CB).*

days 75 and 230)– implies $V_{app} \approx (4.0 \pm 0.4)c$, which, solving for the viewing angle θ in Equation 16, results in $\theta \approx 27.8 \pm 2.9$ deg. This value agrees with $\theta_{GW} = 25 \pm 8$ deg, the angle between the direction to the source and the rotational axis of the binary system, obtained from the gravitational wave observations [51] for the same H_0 [50].

More strikingly, one can invert the order of the previous concordance. If the value of θ_{GW} implied by the GW observations is input in Equation 16, the result is a correct prediction of the magnitude of the observed superluminal velocity. So simple!, this is a “multi-messenger” collaboration working at its best.

7.2. The two superluminally moving sources of GRB030329

This GRB was unique in the sense that it was the subject of a public controversy between advocates and critics of the FB and CB models.

As mentioned in the Introduction, the CB model was used to fit the early AG of GRB030329 and to predict the discovery date of its associated SN, SN2003dh. This being a two-pulse GRB, the fits to its γ rays and to its two-shoulder AG curve consequently involved two cannonballs. The prediction of the amount of their superluminal motions, based on the approximation of a constant ISM density, turned out to be wrong [52]. Subsequent observations of the AG showed a series of very clear re-brightenings, interpreted in the CB model as encounters of the CBs with ISM over-densities [53]. Corrected by the consequent faster slow-down of the CBs’ motion, the new CB-model results were not a prediction, but were not wrong (see [54] and its Figure 2 for many details not mentioned here).

The authors of [52] analyzed their data in terms of a single radio source, in spite of the fact that, with a significance of 20σ , they saw two: *Much less easy to explain is the single observation 52 days after the burst of an additional radio component 0.28 mas northeast of the main afterglow.* Whether there was one or two sources of the AG is the crux of the clash between FB- and CB-model interpretations [54].

Another critique by G. B. Taylor et al. [52] was: *A more general problem for the cannonball model is the absence of rapid fluctuations in the radio light curves of GRB 030329 [55].* That would be true for a sufficiently point-like source, but for CBs it is not correct. For the sake of definiteness, we discuss the issue for this particular GRB:

Initially [40], the radius of a CB in its rest frame is assumed to increase at the speed of sound in a relativistic plasma, $c_s = c/\sqrt{3}$. At an early observer's time T its radius, R , has increased to:

$$R(T, \theta) \approx \frac{c_s}{(1+z)} \int_0^T \delta(t, \theta) dt, \quad (17)$$

where use has been made of the relation between T and the time in the CB's rest system. When the first radio observations started as early as $T = 2.7$ days after burst, the result of Equation 17 for this GRB –for the parameters of the CB-model description of its AG and the deceleration law of Equation 10– is $R(T) \approx 5.7 \times 10^{17}$ cm. This is more than an order of magnitude larger than the largest source size that could still have resulted in diffractive scintillations. Case closed.

To summarize the FB advocates' views on this GRB: Quite forcefully Bloom and collaborators [56] stated: *Very Long Baseline Array imaging of the compact afterglow was used by Frail (2003) [52] to unequivocally disprove the cannonball model for the origin of GRBs.* On the other hand, referring to their “second source” the authors of [52] admitted: *This component requires a high average velocity of $19c$ and cannot be readily explained by any of the standard models. Since it is only seen at a single frequency, it is remotely possible that this image is an artifact of the calibration.*

As for cannonballs, will the dictum *seeing is believing* be rejected, with the time-lapse image of a CB in Figure 11 somehow serving to disprove the cannonball hypothesis ?”

8. Conclusion

The cannonball model provides a successful and very simple and consistent interpretation of SHB170817A. A serious limitation of the model is that the emission of relativistic blobs of matter in core-collapse supernovae and binary-neutron-star mergers is not theoretically well understood. Neither is, in detail, the fate of a CB traveling in the interstellar medium. This is not surprising, for general-relativistic catastrophic magneto-hydrodynamics is not a simple discipline. Hopefully the renewed interest on neutron stars and their mergers provoked by GW170817 will lead to reinvigorated efforts on these subjects.

Acknowledgement

I am indebted to S. Dado, S. L. Glashow and F. Truc for their critical reading of the manuscript. This project has received funding/support from the European Union's Horizon 2020 research and innovation programme under the Marie Skłodowska-Curie grant agreement No 860881-HIDDeN.

References

- [1] B. P. Abbott, et al. (Ligo-Virgo Collaboration), *Nature*, **551**, 85 (2017) [arXiv:1710.05835].
- B. P. Abbott, et al. (Ligo-Virgo Collaboration) *ApJ*, **848**, L13 (2017) [arXiv:1710.05834].
- B. P. Abbott, et al. (Ligo-Virgo Collaboration) *PRL*, **119**, 161101 (2017) [arXiv:1710.05832].
- B. P. Abbott, et al. (Ligo-Virgo Collaboration) *ApJ*, **L12**, 848 (2017) [arXiv:1710.05833].
- [2] J. Hjorth, et al., *ApJ*, **848** L31 (2017), [arXiv:1710.05856].
- [3] J. Goodman, A. Dar, S. Nussinov, *ApJ*, **314**, L7 (1987).
- [4] M. J. Rees, P. Meszaros, *MNRAS*, **25**, 29 (1992).
- [5] S. Dado and A. Dar, arXiv:1708.04603.
- [6] A partial list of reviews include:
T. Piran, *Phys. Rep.* **314**, 575 (1999) [arXiv:astro-ph/9810256].
T. Piran, *Phys. Rep.*, **333**, 529 (2000) [arXiv:astro-ph/9907392].
P. Meszaros, *ARA&A*, **40**, 137 (2002) [arXiv:astro-ph/0111170].
T. Piran *Rev. Mod. Phys.* **76**, 1143 (2004) [arXiv:astro-ph/0405503].
B. Zhang, P. Meszaros, *Int. J. Mod. Phys. A*, **19**, 2385 (2004) [astro-ph/0311321].
P. Meszaros, *Rep. Prog. Phys.* **69**, 2259 (2006) [arXiv:astro-ph/0605208].
B. Zhang, *Chin. J. Astron. Astrophys.* **7**, 1 (2007) [arXiv:astro-ph/0701520].
E. Nakar, *Phys. Rep.* **442**, 166 (2007) [astro-ph/0701748].
E. Berger, *ARA&A*, **52**, 45 (2014) [arXiv:1311.2603].
P. Meszaros, M. J. Rees, (2014) eprint [arXiv:1401.3012].
A. Pe'er, *AdAst*, **Vol. 2015**, 22 (2015) [arXiv:1504.02626].
P. Kumar, B. Zhang, *Phys. Rep.* **561**, 1 (2015) [arXiv:1410.0679].
Z. Dai, E. Daigne, P. Meszaros, *SSRv*, **212**, 409 (2017).
- [7] A. Dar, A. De Rújula, *Phys. Rep.* **405**, 203 (2004) [arXiv:astro-ph/0308248].
Kee ideas underlying the CB model were adopted from:
N. J. Shaviv, A. Dar, *ApJ*, **447**, 863 (1995) [arXiv:astro-ph/9407039].
A. Dar, *ApJ*, **500**, L93 (1998) [arXiv:astro-ph/9709231].
A. Dar *A&AS*, **138**, 505 (1999) [arXiv:astro-ph/9902017].
A. Dar, R. Plaga, *A&A* **349**, 259 (1999) [arXiv:astro-ph/9902138].
A. Dar, A. De Rújula, 2000 e-print [arXiv:astro-ph/0012227].
S. Dado, A. Dar, A. De Rújula, *A&A*, **388**, 1079D (2002) [arXiv:astro-ph/0107367].
- [8] S. Dado and A. Dar, [arXiv:1810.03514].
See also S. Dado, A. Dar, A. De Rújula, [arXiv:2204.04128].
- [9] N. J. Shaviv, A. Dar, *ApJ*, **447**, 863 (1995) [arXiv:astro-ph/9407039].
A. Dar, A. De Rújula, *Phys. Rept.* **405**, 203 (2004) [arXiv:astro-ph/0308248].
- [10] S. Dado, A. Dar and A. De Rújula, *Astrophys.J.Lett.* **594**, L89 (2003) [astro-ph/0304106].
- [11] S. Dado, A. Dar, A. De Rújula, *A&A*, **388**, 1079 (2002) [arXiv:astro-ph/0107367].
S. Dado, A. Dar, A. De Rújula, *ApJ*, **646**, L21 (2006) [arXiv:astro-ph/0512196].
- [12] S. Vaughan, et al., *ApJ*, **638**, 920 (2006) [arXiv:astro-ph/0510677].
- [13] G. Cusumano, et al., *ApJ*, **639**, 316 (2006) [arXiv:astro-ph/0509689].
- [14] A. Dar and A. De Rújula, [arXiv:astro-ph/0012227].
- [15] S. Dado, A. Dar and A. De Rújula, *Astrophys. J.* **663**, 400 (2007).
- [16] S. Dado, A. Dar, *A&A*, **558**, A115 (2013) [arXiv:1303.2872].
- [17] S. Dado, A. Dar, *PRD*, **99**, 123031 (2019) [arXiv:1807.08726]. For earlier ideas how the spin-down of newly born millisecond pulsars powers the early time AG of GRBs, see reference [18].
- [18] E. G. Blackman, I. Yi, *ApJ*, **498**, L31 (1998) [arXiv:astro-ph/9802017].
Z. G. Dai, T. Lu, *PRL*, **81**, 4301 (1998) [arXiv:astro-ph/9810332].

- Z. G. Dai, T. Lu, A&A, **333**, L87 (1998) [arXiv:astro-ph/9810402].
 B. Zhang, P. Meszaros, ApJ, **552**, L35 (2001) [arXiv:astro-ph/0011133].
 Z. G. Dai et al., Science, **311**, 1127 (2006), [arXiv:astro-ph/0602525].
 B. D. Metzger, E. Quataert, T.A. Thompson, MNRAS, **385**, 1455 (2008) [arXiv:0712.1233].
 B. P. Gompertz, P.T. O'Brien, G.A. Wynn, MNRAS, **438**, 240 (2014) [arXiv:1311.1505].
 A. Rowlinson, et al., MNRAS **409**, 531 (2010) [arXiv:1007.2185].
 B. D. Metzger, A. L. Piro, MNRAS, **439**, 3916 (2014) [arXiv:1311.1519].
 H. Lu, et al., MNRAS, ApJ, **805**, 89 (2015) [arXiv:1501.02589].
 S. Gibson, et al., MNRAS, **470** 4925 (2017) [arXiv:1706.04802].
- [19] L. Amati, F. Frontera, M. Tavani, et al., A&A, **390**, 81 (2002) [arXiv:astro-ph/0205230].
 [20] The Gamma Ray Coordinates Network, <https://gc.n.ssf.nasa.gov/>
 [21] See, e.g. W. C. Straka and C. J. Lada, ApJ., 195, 563 (1975) and references therein.
 [22] For LGRBs, see, e.g., S. Dado, A. Dar, A. De Rújula, ApJ, **696**, 994 (2009) [arXiv:0809.4776].
 For SGRBs, see e.g., S. Dado, A. Dar, 2018 e-print [arXiv:1808.08912].
 [23] A. Goldstein, et al., ApJ, **848**, L14 (2017) [arXiv:1710.05446].
 [24] A. Dar, S. Dado and A. De Rújula, to be published.
 [25] K. P. Mooley, et al., Nature, **561**, 355 (2018) [arXiv:1806.09693].
 [26] A. von Kienlin, et al., 2017, GCN Circular 21520.
 [27] A. Goldstein, et al., ApJ, **848**, L14 (2017) [arXiv:1710.05446].
 [28] A. S. Pozanenko, et al., ApJ, **852**, 30 (2018) [arXiv:1710.05448].
 [29] V. Savchenko, et al., ApJ, **848**, L15 (2018) [arXiv:1710.05449].
 [30] Goldstein, A., et al. 2017, GCN Circular 21528.
 [31] A. Goldstein, et al., ApJ, **848**, L14 (2017) [arXiv:1710.05446].
 [32] E. E. Fenimore, C. D. Madras, S. Nayakshin, AJ, **473**, 998 (1996) [arXiv:astro-ph/9607163].
 P. Kumar, A. Panaitescu, 2000, ApJ, **541**, L51 (2000), [arXiv:astro-ph/0006317].
 F. Ryde, V. Petrosian, AJ, **578**, 290 (2002), [arXiv:astro-ph/0206204].
 D. Kocevski, F. Ryde, E. Liang, ApJ, **596**, 389 (2003) [arXiv:astro-ph/0303556].
 C. D. Dermer, ApJ, **614**, 284 (2004) [arXiv:astro-ph/0403508].
 E. W. Liang, et al., ApJ, **646**, 351 (2006) [arXiv:astro-ph/0602142].
 A. Panaitescu, NC, **B121**, 1099 (2006) [arXiv:astro-ph/0607396].
- [33] S. Kobayashi, T. Piran, R. Sari, ApJ, **490**, 92 (1997) [arXiv:astro-ph/9705013].
 [34] J. P. Norris, et al., ApJ, **627**, 324 (2005) [arXiv:astro-ph/0503383].
 J. Hakkila, et al., ApJ, **815**, 134 (2015) [arXiv:1511.03695].
 [35] S. Dado, A. Dar, Phys. Rev. **D101**, 063008 (2019), arXiv:1907.10523.
 [36] S. Dado, A. Dar, ApJ, **855**, 88 (2018) [arXiv:1710.02456] and references therein.
 [37] Swift-XRT GRB light curve repository, UK Swift Science Data Centre, Univ. of Leicester:
 P. A. Evans, et al., A&A, **469**, 379 (2007) [arXiv:0704.0128].
 P. A. Evans, et al., MNRAS, **397**, 1177 (2009) [arXiv:0812.3662].
 [38] M. R. Drout, et al., Science, **358**, 1570 (2017) [arXiv:1710.05443].
 [39] S. Makhathini et al. 2011, arXiv:2006.02382v3.
 [40] A. Dar and A. De Rújula, Phys.Rept. **466**, 179 (2008).
 [41] K. P. Mooley, et al., ApJ, **868**, L11 (2018) [arXiv:1810.12927].
 [42] K. P. Mooley, et al., ApJ, **868**, L11 (2018), [arXiv:1810.12927].
 [43] K. P. Mooley, et al., Nature, **554**, 207 (2018) [arXiv:1711.11573V1].
 [44] D. Dobbie et al. ApJ **858**, L15 (2018) [arXiv:1803.06853V3].
 [45] D. Lazzati, et al., e-print arXiv:1712.03237v1 (2017).
 [46] D. Lazzati, et al., PRL, **120** 241103 (2018) [arXiv:1712.03237v4].
 [47] J.C. Kapteyn, 1902, Astron. Nachr., **157** 201 (1902).
 [48] P. Courdec, Annales d'Astrophysique **2**, 271 (1939)
 M. J. Rees, Nature, **211**, 468 (1966).
 [49] A. Dar, A. De Rújula, 2000, e-print arXiv:astro-ph/0008474.
 S. Dado, A. Dar, A. De Rújula, 2016, e-print [arXiv:1610.01985].
- [50] A. G. Riess, et al., ApJ, **826** 56 (2016) [arXiv:1604.01424].
 A. G. Riess, et al. ApJ, **861**, 126 (2018) [arXiv:1804.10655].
 [51] I. Mandel, ApJ, **853**, L12 (2018), [arXiv:1712.03958]. See Table 1.
 S. Nissanke, et al., ApJ, **725**, 496 (2010) [arXiv:0904.1017].
 [52] G. B. Taylor, et al., ApJ, **609**, L1 (2004) [arXiv:astro-ph/0405300v1].
 [53] S. Dado, A. Dar and A. De Rújula, astro-ph/0402374
 [54] S. Dado, A. Dar and A. De Rújula, astro-ph/0406325.
 [55] Berger E. et al., Nature, **426**, 154 (2003).
- [56] J.S. Bloom et al. The Astronomical Journal **127**, 252-263 (2003), [astro-ph/0308034].